Analytical Application of Modified Hollow Cathode Lamp with Planar Solid Sample

Kazuaki WAGATSUMA and Kichinosuke HIROKAWA

Institute for Materials Research, Tohoku University, Katahira, Sendai 980

A modified hollow cathode discharge lamp having three electrodes, which is operated with two individual power sources, has been developed for elemental analyses. The lamp enables analyte atoms to be directly introduced from a planar sample into the hollow cathode plasma. Detection limits and spectral interferences are reported for minor alloyed elements in various Fe-matrix alloys.

Keywords Hollow cathode discharge lamp, atomic emission spectrometry, iron-based alloys

The hollow cathode discharge lamp has been widely employed as a light source for atomic absorption spectrometry. The properties of narrow width of the spectral lines, high intensity, and stability of the discharge have made it a source usually suitable for this purpose. In atomic emission spectrometry, many investigators have also reported the spectroscopic characteristics[1-3] or analytical applications[1-6] of the discharge lamp. The method in which solution samples have been inserted into the hollow cathode has been described in previous studies because of the restrictions on the cathode shape.

An analytical application of a dual-cathode glow discharge tube was investigated and is discussed here. The lamp consists of three electrodes: anode, intermediate electrode, and cathode (sample) (*cf.* Fig. 1). The hollow cathode plasma (HCP) is generated in the cylindrical, hollow intermediate electrode and the sample atoms are sputtered into the plasma from the cathode with the aid of a bias voltage supply. Therefore, the sample may have the shape of a plate or a block.

A Grimm-type glow discharge (Grimm-GD) lamp[7] has been used to analyze solid sample surfaces. It has been reported that, depending on the kind of the sample, the voltage–current characteristics are drastically varied[8], and thus, it is difficult to keep the sputtering and/or the excitation conditions constant for various samples. This effect implies that the discharge conditions must be predetermined for materials measured with the Grimm-GD lamp. The HCP created in our lamp is principally controlled by the voltage supplied between the anode and the intermediate electrode. Therefore, a stable discharge plasma can be obtained, independent of the kind of the cathode material (sample). The bias voltage can be supplied to regulate the sample atom introduced into the HCP without influencing the HCP discharge conditions.

Direct analyses of solid samples are attempted for minor alloyed elements in several Fe-matrix alloys. In this paper, detection limits and spectral interferences for some analytical emission lines are reported.

Experimental

Discharge lamp

Figure 1 shows a cross section of the discharge lamp schematically illustrated. The lamp comprises an anode, an intermediate electrode, and a cathode (sample). These electrodes are isolated with PTFE insulators. The intermediate electrode can be easily demounted and interchanged. The anode, the intermediate electrode,

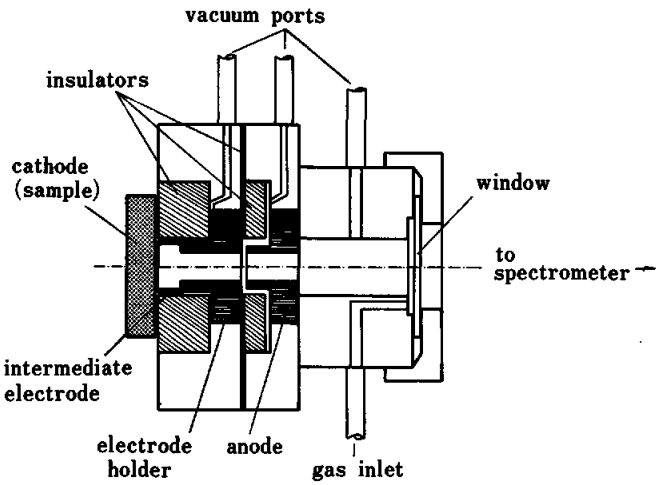

Fig. 1 Schematic cross-section diagram of hollow cathode discharge lamp.

and the housing of the lamp are made from copper–zinc alloy (α-brass). The side of the intermediate electrode adjacent to the cathode sample is 11.0 mm in diameter and the other side is 8.0 mm in diameter. The inner diameter of the hollow anode is 8.0 mm. The distance between the anode and the intermediate electrode is adjusted to be about 1.0 mm and that between the intermediate electrode and cathode to be about 0.1–0.2 mm. The lamp is evacuated to 4.0–2.0 Pa by oil rotary pumps and then pure argon gas (more than 99.9995% purity) is introduced to flow continuously during the measurement. The gas pressure is regulated with a needle valve and is read on a Pirani gauge at the vacuum port of the lamp.

Apparatus

A schematic diagram of our apparatus is illustrated in Fig. 2. The hollow cathode discharge plasma which is created in the intermediate electrode results from a pulsed voltage supplied between the anode and intermediate electrode. The wave pattern of the pulsed voltage is a rectified half-sine wave form. The discharge voltage is generated with a bipolar power amplifier (Kikusui Electronics Co., POW 70–2 model), a step-up transformer, and a silicon diode. The bipolar amplifier is regulated by a signal generator (NF Electronics Co., E–1202 model) and the frequency and the amplitude of the pulsed voltage are predetermined.

Apart from the power source for the hollow cathode plasma, a bias voltage is supplied between the intermediate electrode and the cathode with a dc power supply (Kikusui Electronics Co., PAD 1K–0.2L model). The bias voltage will control the sputtering process of sample atoms (from the cathode surface into the hollow cathode plasma).

Spectral signals emitted from the plasma could be modulated at the frequency of the pulsed discharge. The radiation is dispersed and detected on a grating spectrometer (Hitachi, 808 model). The resultant signals are amplified with a pre-amplifier and then recorded with a lock-in amplifier (NF Electronics Co., LI–574A model).

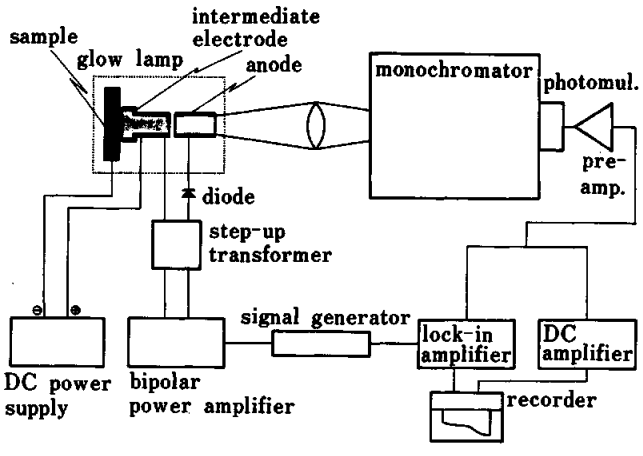

Fig. 2 Block diagram of the apparatus.

Samples

The series of Fe-matrix alloy samples was received from the Iron and Steel Institute of Japan (standard samples for X-ray fluorescence analysis). Several binary (Fe–X) or ternary (Fe–X–Y) alloys were employed to determine the alloyed elements (X or Y). The surfaces were mechanically polished with waterproof emery papers. Pre-discharges for more than 10 min were carried out to remove the surface contaminations on the sample or the inside wall of the intermediate electrode. The sputter crater is estimated to be *ca.* 10 mm in diameter.

Results and Discussion

The average current (or voltage) and the frequency of the pulsed discharge, the pressure of argon gas, and the bias voltage play significant roles in determining the excitation of emission lines and the sputtering conditions. The discharge current can effectively control the discharge conditions of the hollow cathode discharge plasma. The bias voltage between the intermediate electrode and cathode is expressed as a negative potential when the intermediate electrode is grounded (0 V).

Figure 3 shows the relation between emission intensities of three neutral iron lines: Fe I 372.0, Fe I 374.6, and Fe I 386.0 nm, and the average current of the pulsed hollow cathode discharge when an iron plate is used as the cathode sample. Clearly, the emission intensities monotonously increase with the discharge currents. Emission intensities of Ar II spectral lines are

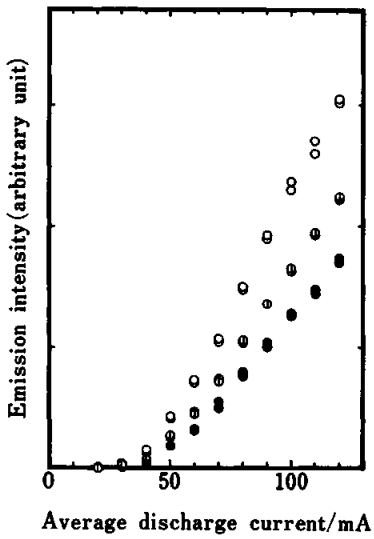

Fig. 3 Variations of Fe I emission intensities as a function of average discharge current of hollow cathode plasma. Iron emission lines: ○, 372.0 nm; ⊙, 386.0 nm; ●, 374.6 nm. Ar pressure, 2.7×10^2 Pa (fixed); frequency of hollow cathode discharge, 270 Hz; bias voltage: 0 V (equal potential between intermediate electrode and cathode).

also raised at higher discharge currents when they are recorded under the same discharge conditions as used with Fig. 3. This fact implies that the density of excited Ar^+ species in the plasma becomes higher as the discharge currents are raised. However, the Ar II emission intensities change little with a variation in the bias voltage, as described later. These results suggest that the discharge currents principally control the population of Ar^+ ions in the lamp, thus indicating that the Ar^+ ions are produced mainly in the hollow cathode plasma. The number of argon ions which impinge on the cathode surface determines the number of the sputtered iron atoms. Therefore, the emission intensities of the Fe I lines would strongly depend on the discharge current of the hollow cathode plasma.

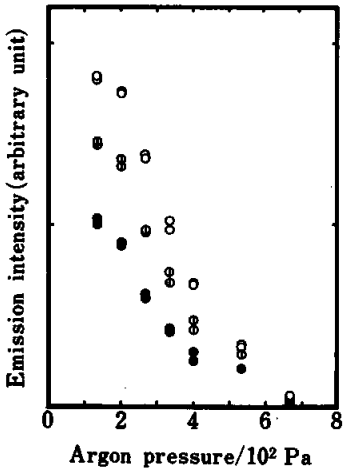

Fig. 4 Plots of Fe I emission intensities against Ar pressures. Iron lines, see Fig. 3; average discharge current, 80±1 mA; frequency, 270 Hz; bias voltage, 0 V.

Figure 4 shows that the Fe I emission intensities drastically increase at lower Ar pressures when the average discharge current of the plasma is kept at 80±1 mA. When the discharge current is maintained constant, the discharge voltage is also higher at lower Ar pressures. Furthermore, increased emission intensities of the Ar II lines can be observed with a reduction in the pressure of argon gas. Thus, at reduced gas pressures, the sputter rates would increase because of the higher density and higher kinetic energy of the projectiles (Ar^+ ions).

Figure 5 indicates plots of the Fe I emission intensities against the bias voltage when the discharge current of the plasma and the Ar pressure are fixed at 80±1 mA and 2.7×10^2 Pa. The negative bias voltage supplied between the intermediate electrode and the sample causes the argon ions to be drawn to and to accelerate toward the sample surface from which the sputtered particles are ejected. Therefore, high bias voltage could contribute to an increase in the number of the sputtered atoms. However, little variation in the Ar II emission intensities is observed, independent of the bias voltages, as shown in Fig. 6. The bias voltages (which vary in the range from 0 to −200 V) have little influence on the Ar II emission, whereas the Fe I intensities are noticeably controlled by the bias voltages. It appears plausible that the population of Ar^+ excited species would be insensitive to relatively small variations in the bias voltages due to their high excitation energies (more than 19 eV).[9] However, the sputter rates could be directly susceptible to the change in the bias voltages. Accordingly, only the Fe I emission intensities would increase with the bias voltages.

The dependence of the Fe I emission intensities on the frequency of the pulsed discharge was also investigated. Even though the other conditions are kept the same, these intensities achieve maximum values at

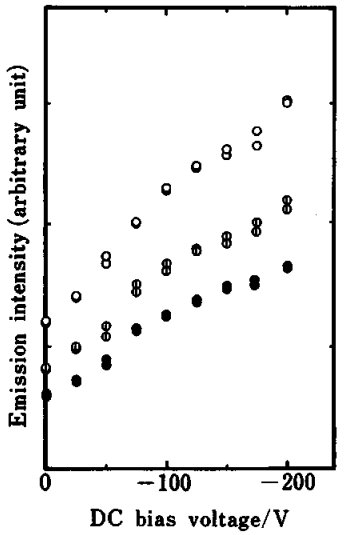

Fig. 5 Effects of bias voltage on Fe I emission intensities. Iron lines, see Fig. 3; Ar pressure, 2.7×10^2 Pa (fixed); average discharge current, 80±1 mA (fixed); frequency, 270 Hz.

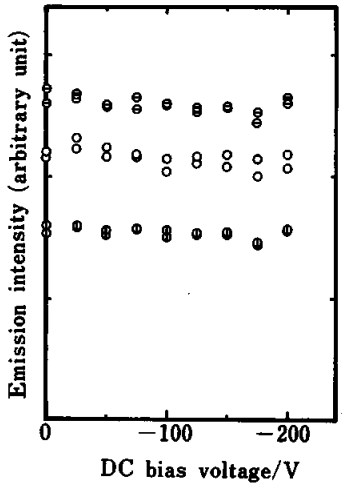

Fig. 6 Effects of bias voltage on emission intensities of some Ar II lines. Argon lines: ⊖, 461.0 nm; ○, 454.5 nm; ⊙, 459.0 nm. The discharge conditions are the same as those used with Fig. 5.

Table 1 Operating conditions of the lamp for elemental analysis

Argon pressure	2.7×10^2 Pa (2 Torr)
Discharge current	135±2 mA
Frequency of discharge	135 Hz
Bias voltage	−250 V
Integration time	60 s

Table 2 Detection limits for analytical emission lines measured with various Fe-matrix binary alloys

Analytical line	Detection limit	
	wt.%	at.%
Al I 396.1 nm	4.0×10^{-4}	8.7×10^{-4}
Cr I 425.4 nm	4.5×10^{-4}	5.1×10^{-4}
Cr I 428.9 nm	8.6×10^{-4}	9.7×10^{-4}
Mn I 403.1 nm	5.4×10^{-4}	5.8×10^{-4}
Ni I 341.5 nm	3.9×10^{-3}	3.9×10^{-3}
Ti I 365.3 nm	2.0×10^{-3}	2.5×10^{-3}
V I 439.0 nm	3.8×10^{-3}	3.4×10^{-3}
Co I 350.2 nm	6.6×10^{-3}	6.6×10^{-3}
Mo I 386.4 nm	4.4×10^{-3}	2.7×10^{-3}
Mo I 313.2 nm	8.3×10^{-3}	5.1×10^{-3}
W I 400.9 nm	1.5×10^{-3}	4.8×10^{-3}

frequencies of 100 - 200 Hz and then gradually reduce with an increase in the frequency. However, the Ar II emission intensities seem to be independent of the discharge frequency. Therefore, the sputtering process would be unable to follow a switching occurring in the plasma as the frequency of the pulsed discharge increases, though the detailed mechanisms are not yet obvious.

The operating conditions are selected to obtain the maximum sensitivity, as summarized in Table 1. As already shown in Fig. 4, the strongest emission intensities are provided at 1.3×10^2 Pa Ar, assuming that the other discharge conditions are the same. However, the stability of the emission intensities has a tendency to become worse as the Ar pressure is reduced. Therefore, the pressure of argon gas was set to be 2.7×10^2 Pa. More intense Fe I emission can be observed as the discharge current becomes higher. The output power of the bipolar power amplifier restricts the available discharge current. At higher bias voltages, the emission intensities of the Fe I lines also increase. However, the hollow cathode discharge becomes unstable at bias voltages of more than *ca.* 280 V (at the Ar pressure of 2.7×10^2 Pa).

As shown in Table 2, analytical lines are selected for each element analyzed. The spectroscopic features of these emission lines, which have the excitation energy

Table 3 Spectral interferences of high alloyed elements in Fe-matrix alloys to analytical emission lines

Analytical line	Spectral interference[a]		
	Fe–25wt%Ni	Fe–25wt%Cr	Fe–20wt%W
Al I 396.1 nm	N	N	N
Cr I 425.4 nm	NS	—	NS
Cr I 428.9 nm	N	—	NS
Mn I 403.1 nm	‡	N	NS
Ni I 341.5 nm	—	N	N
Ti I 365.3 nm	NS	NS	NS
V I 439.0 nm	N	NS	N
Co I 350.2 nm	N	N	N
Mo I 386.4 nm	N	N	N
Mo I 313.2 nm	(Ni I 313.4)	N	NS
W I 400.9 nm	N	N	—

a. Symbols: N, none; NS, negligibly small; ‡, unknown because Fe–25wt% Ni alloy contains 0.36wt% Mn.
Concentration tolerance of interfering elements: (interfering/analyte element), N, more than 10^2; NS, $10^2 - 10^3$.

of 3 - 4 eV[10], are similar to those of the Fe I lines presented in Figs. 3 - 5. The calibration factors of various Fe–X binary alloy systems are estimated for each analytical line. Detection limits expressed as weight% (atomic%) of X element in the Fe-matrix alloys, based on twice the average value of the background fluctuation, are given in Table 2. The background fluctuation levels are measured with a pure iron sample for the wavelength of each analytical line. Nickel, chromium, and tungsten may be added as major alloyed elements in stainless steels or tool steels. Table 3 indicates the spectral interferences of these elements to the analytical lines listed in Table 2. It can be seen that the interferences are negligibly small in the determination of the minor alloyed elements in Fe-matrix alloys.

References

1. R. Mavrodineau, *J. Res. Natl. Bur. Stand.*, **89**, 143 (1984).
2. J. A. C. Broekaret, *J. Anal. Atom. Spectrom.*, **2**, 537 (1987).
3. S. Caroli, *J. Anal. Atom. Spectrom.*, **2**, 661 (1987).
4. W. W. Harrison and E. H. Daughtrey, *Anal. Chim. Acta*, **65**, 35 (1973).
5. W. W. Harrison and N. J. Prakash, *Anal. Chim. Acta*, **49**, 151 (1970).
6. H. G. C. Human, P. J. T. Zeegers and J. A. van Elst, *Spectrochim. Acta*, **29B**, 111 (1974).
7. W. Grimm, *Spectrochim. Acta*, **23B**, 443 (1968).
8. P. W. J. M. Boumans, *Anal. Chem.*, **44**, 1219 (1972).
9. K. Wagatsuma and K. Hirokawa, *Anal. Chem.*, **57**, 2901 (1985).
10. K. Wagatsuma and K. Hirokawa, *Anal. Chem.*, **56**, 908 (1984).

(Received November 5, 1987)
(Accepted January 21, 1988)